

3D MR image analysis of the developing human fetal brain from in utero clinical studies

Colin Studholme

Associate Professor in Residence

Biomedical Image Computing Group
<http://radiology.ucsf.edu/bicg>

Department of Radiology & Biomedical Imaging,
University of California San Francisco
Bioengineering Graduate Group
UCB/UCSF



1

Fetal Brain Imaging: Mapping Normal Development and detecting early abnormality



- Standard Clinical Tool: Ultrasound imaging
 - Noninvasive, relatively low cost, fast
 - Reveals main tissue boundaries
 - But: Cannot easily delineate soft tissue characteristics
- Fetal MR imaging
 - Recently emerged as a safe tool to image the developing fetus
 - Patients referred after Ultrasound scan picks up abnormality
 - MRI Provides high resolution and tissue contrast
 - Detects fine scale structure, subtle tissue abnormalities
eg grey/white matter, lesions

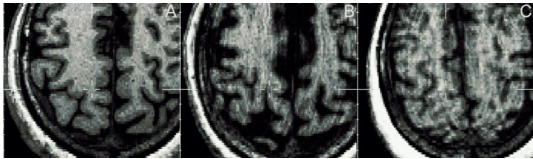
2

Fetal MRI vs Adult MRI



- Adults (generally) can be told to remain still during an MRI study
- Fetuses move and (generally) respond less well to requests than adults
 - Smaller fetuses have more space and move more
- Typical 3D adult structural MRI scans take 2-12min
 - Motion artifacts occur if head motion during study
- To acquire full 3D MR image during motion without significant artifact:
 - whole study would have to take fraction of a second

Adult 3D MR Imaging with motion



3

Approaches to Clinical Fetal Imaging



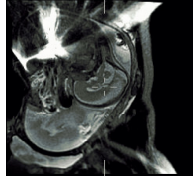
- Faster 3D MR Imaging techniques available:
 - Eg 3D EPI
 - But: These do not provide clinically optimal tissue contrast AND still not fast enough
- Motion correction for 3D imaging:
 - Acquisition (navigator echoes) and retrospective K-space correction techniques
 - Generally assume rigid object surrounded by air
 - Fetus: rigid head surrounded by deforming tissues
- Solution: Current Clinical Fetal Imaging -> 2D multi slice
 - Each slice takes < 0.5 sec

4

Example Clinical Images

UCSF

- T2W Multi Slice
 - Single shot fast spin echo (SSFSE; 2D)
 - T2 weighted (1/2 sec/frame)
 - TR = 6000 ms, TE = 90 ms
 - Approximately 0.5x0.5x3 mm³ voxel dimension
 - 15-30 slices in each stack

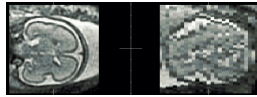


- Anisotropic resolution with thick slices

- Fetal motion during study:
 - Fetal motion commonly occurs between slices,
 - Set of 2D slices not consistent geometrically in 3D,
 - Missing portions of the underlying anatomy in a given stack.

- Intensity distortion between scans:
 - Inhomogeneous sensitivity of the coil over FOV
 - Fluid/Air boundaries in Maternal Anatomy:
 - Distortion because: Susceptibility and Motion

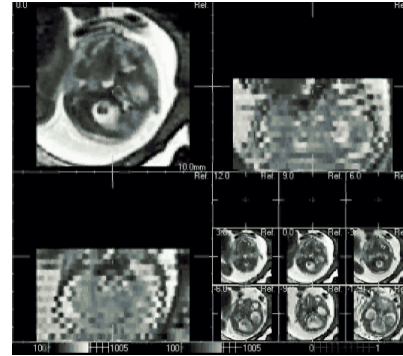
coronal slice slice stack



5

Fetal Motion in Multi Slice SSFSE

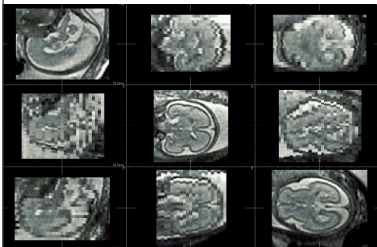
UCSF



6

Aim

UCSF



Single
High resolution
volume

- We would like to Compound several acquisitions,
- We need to Correct fetal motion,
- and Correct relative intensity distortions.

7

Reconstruction Based Slice Alignment

Francois Rousseau, PhD
Postdoc 2003-2005

F. Rousseau, O. A. Glenn, B. Iordanova, C. E. Rodriguez-Carranza, D. Vigneron, J. A. Barkovich, and C. Studholme, "A novel approach to high resolution fetal brain MR imaging," in Medical Image Computing and Computer-Assisted Intervention, LNCS, vol. 3749, pp. 548-555, October 2005.

F. Rousseau, O. A. Glenn, B. Iordanova, C. E. Rodriguez-Carranza, D. B. Vigneron, A. J. Barkovich, and C. Studholme, "Registration-based approach for reconstruction of high-resolution in utero MR brain images," Acad. Radiol., vol. 13, no. 9, pp. 1072-1081, September 2006.

8

Reconstruction Based Slice Motion Correction

- Initial Global Rigid Stack Alignment
 - Ignoring individual slice motion
- Form a single Image Volume on Regular rectangular lattice
 - Using an reconstruction method (Scattered Data Interpolation)
- Match Groups/Individual Slices to Reconstructed Volume

9

Hierarchical Slice Registration: Multi-resolution Accounting for Spatio-Temporal Order of Acquisition

Spatially: Odd slices in stack acquired
Then even slices are acquired

(A) 1 group (B) 2 groups (C) 4 groups (D) 8 groups (E) 16 groups

- A Stack Level Registration
- B Interleave Level Registration
- C-E interleaves further divided into two, until individual slice based alignment

10

Slice to Volume Alignment

- Maximize Similarity Measure between 3D volume and slice:
 - Normalized Mutual Information of image intensities
$$h(A), h(B) : \text{marginal entropies, } h(A,B) : \text{joint entropy}$$

$$NMI(A, B) = \frac{h(A) + h(B)}{h(A, B)}$$
- 'Multi-modality' criteria that allows differences in structure and contrast

Reconstructed Volume
Before slice alignment

- 3D Rigid Transformations:
Full 3D fetal head motion allowed between slices

11

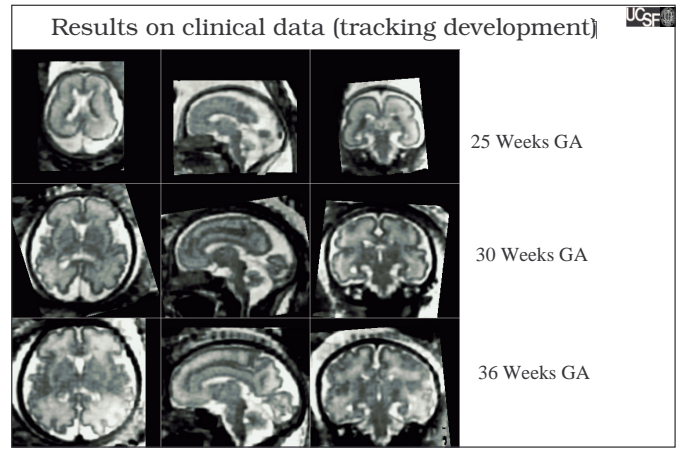
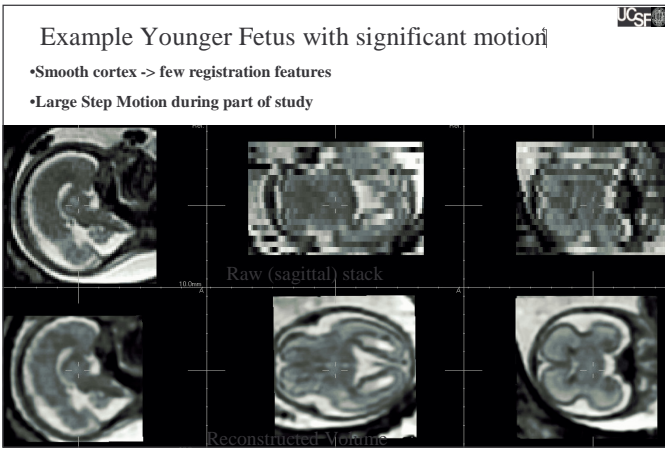
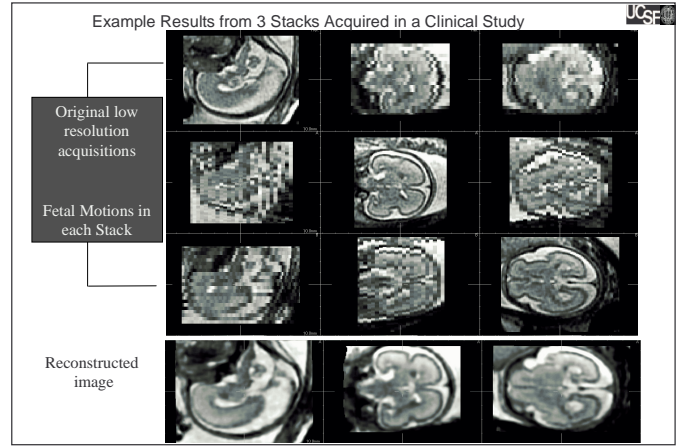
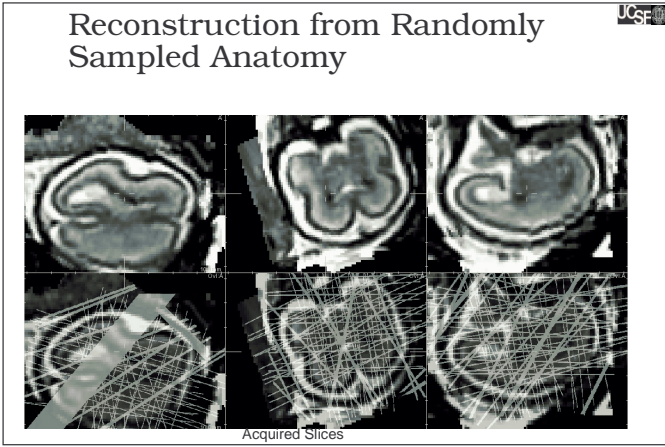
Volume Reconstruction

- 3D Reconstruction from Scattered Data:
 - Local neighborhood approach : Anisotropic Gaussian Kernel (orientated with the slices).
- Relative Intensity Correction between slices
 - Remove Slowly varying (spatial) differences in image contrast
- Algorithm :
 - One image stack is chosen as a reference,
 - Assume: Multiplicative distortion, varying smoothly over the image
 - Correction of a stack to reference is estimated from low pass filtered images :

$$\beta_i(x) = a_i * \frac{\mathcal{G}(IR(x))}{\mathcal{G}(I_{LR}^i(x))} \quad \text{with } a_i = \frac{\sum_x I_{LR}^i(x)}{\sum_x I_{LR}^1(x) \frac{\mathcal{G}(IR(x))}{\mathcal{G}(I_{LR}^1(x))}}$$

$$I_{LR}^i(x) = \beta_i(x) I_{LR}^1(x)$$

12

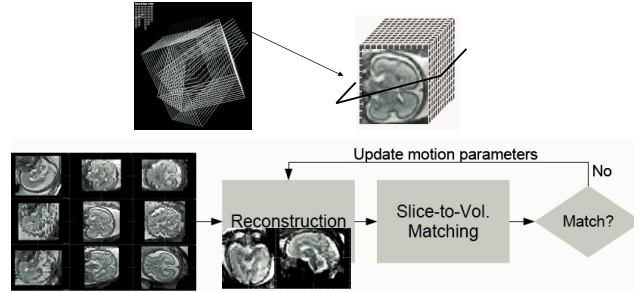


Intersection Based Slice Alignment

Kio Kim PhD

K. Kim, M. F. Hansen, P. A. Habas, F. Rousseau, O. A. Glenn, A. J. Barkovich, and C. Studholme, "Intersection-based registration of slice stacks to form 3D images of the human fetal brain," in Proc. 5th IEEE International Symposium on Biomedical Imaging: From Nano to Macro, pp. 1167-1170, May 2008.

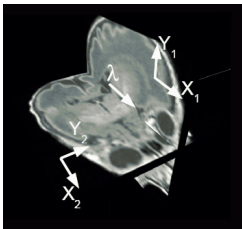
Slice to Volume Alignment



- Two Step Process: 3D reconstruction and slice-to-volume alignment
- No global or even local convergence guaranteed
- Final registration accuracy limited by blurring in reconstruction

Intersection Based Slice Alignment

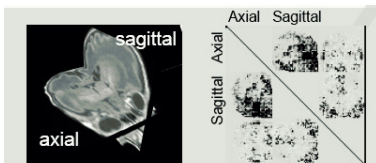
Consider Direct Match of Any Pair of Slices



Dissimilarity is measured directly by sum of squared difference in intensity along intersection

$$D_{ij} \equiv \frac{1}{|I_i \cap I_j|} \int_{I_i \cap I_j} \|I_i(x_{ij}(\lambda; \theta_i, \theta_j)) - I_j(x_{ji}(\lambda; \theta_j, \theta_i))\|^2 d\lambda$$

I_i : The i -th image slice
 θ_i : Motion parameters of the i -th image slice
 x_j : Position vector of the intersection segment in slice i against slice j



∂D w.r.t. X -displacements of an axial slice is negatively correlated to that of a sagittal slice.

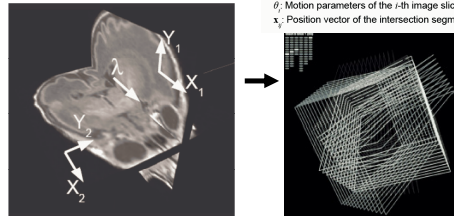
Relationship between slices: Each slice Influences the location of all others



- Location of each slice influences match with all other intersecting slices

$$D_{ij} \equiv \frac{1}{|I_i \cap I_j|} \int_{I_i \cap I_j} \|I_i(x_{ij}(\lambda; \theta_i, \theta_j)) - I_j(x_{ji}(\lambda; \theta_j, \theta_i))\|^2 d\lambda$$

I_i : The i -th image slice
 θ_i : Motion parameters of the i -th image slice
 x_j : Position vector of the intersection segment in slice i against slice j



- Matches are all interrelated:
Need to resolve relative collective alignment simultaneously

Relationship between slices: Each slice Influences the location of all others

$D_{ij} = \frac{1}{|I_i \cap I_j|} \int_{I_i \cap I_j} \|I_i(x_{ij}(\lambda, \theta_i, \theta_j)) - I_j(x_{ij}(\lambda, \theta_j, \theta_i))\|^2 d\lambda$
 i, j : The i -th image slice
 θ : Motion parameters of the i -th image slice
 x_{ij} : Position vector of the intersection segment in slice i against slice j

Iterative Parameter Update Used:
 $\Theta^{k+1} = \Theta^k - [2(\nabla_{\Theta} D)^T \nabla_{\Theta} D + \alpha I]^{-1} \nabla_{\Theta} E$
 $\frac{\partial D}{\partial \theta'} = \sum_{i,j} \left(\frac{\partial x_{ij}}{\partial \theta'} \right)^T \nabla_{x_{ij}} D$

$D(\Theta)$: Lexicographical representation of differences between all intersection profiles, given the motion parameters Θ

∂D w.r.t. x -displacements of an axial slice is negatively correlated to that of a sagittal slice.

Covariance matrix of intersection profiles

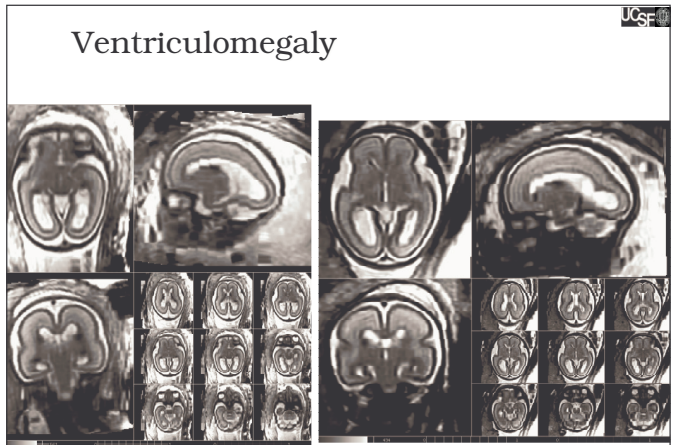
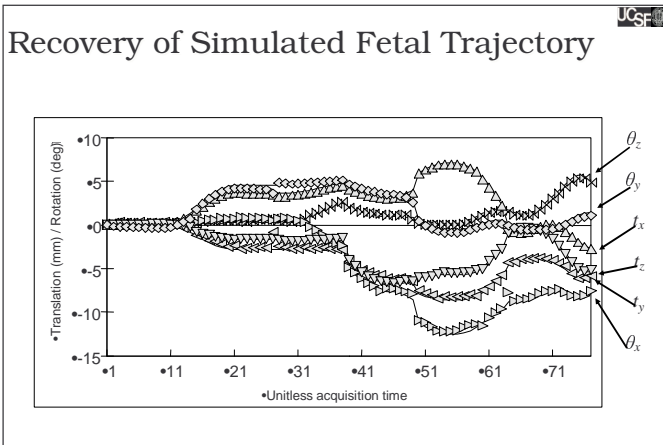
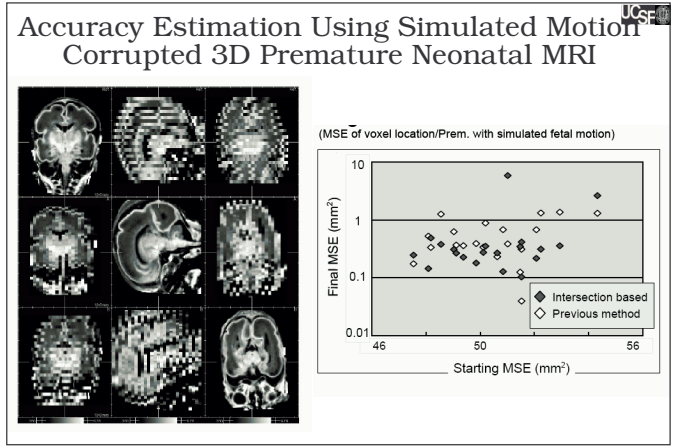
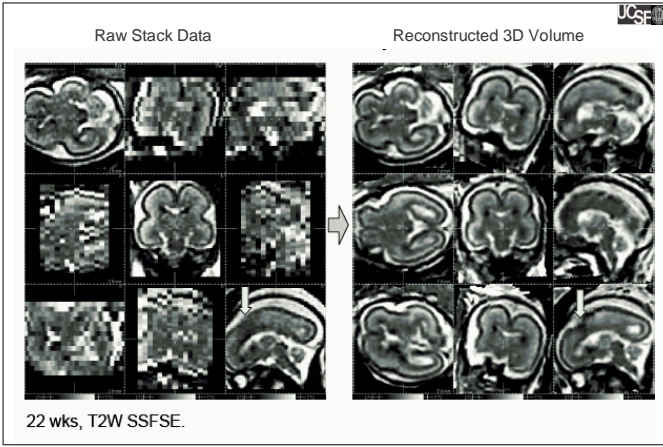
Hierarchical Slice Registration: Multi-resolution Accounting for Spatio-Temporal Order of Acquisition

- A Stack Level Registration
- B Interleave Level Registration
- C-E interleaves further divided into two, until individual slice based alignment

Raw Stacks

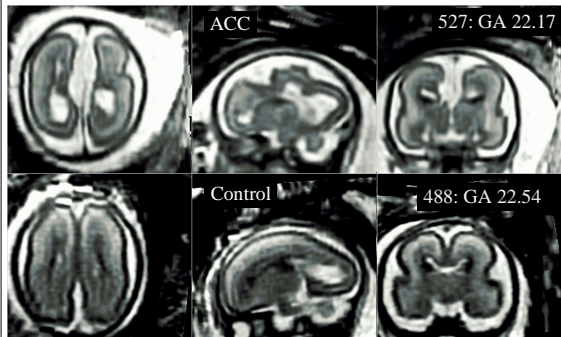
With slice alignment

Axial Sagittal Coronal Reconstructed 3D



Agenesis of the Corpus Callosum

JCSF



29

Segmentation of Developing and Transient Tissue Types in Fetal MRI.

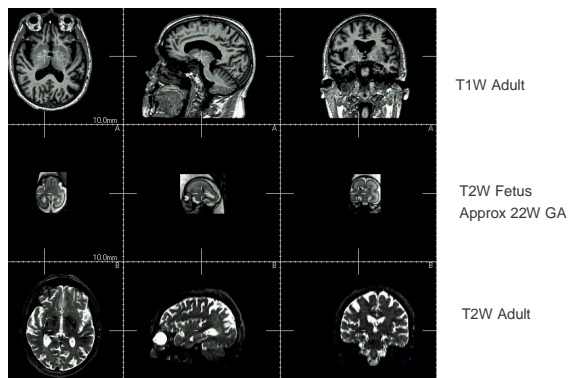
Piotr Habas, PhD

P. A. Habas, K. Kim, F. Rousseau, O. A. Glenn, A. J. Barkovich, and C. Studholme, "Atlas-based segmentation of the germinal matrix from in utero clinical MRI of the fetal brain," in Medical Image Computing and Computer-Assisted Intervention, LNCS, vol. 5241, part I, pp. 351-358, September 2008.

30

T2W Fetal MRI

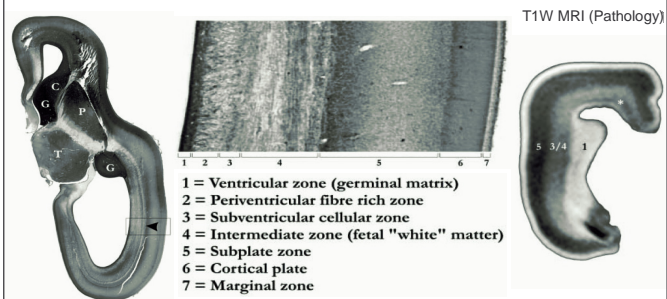
JCSF



31

Laminar organization of the fetal brain

JCSF



[Kostovic et al, Cerebral Cortex, 2002, 536-544]

32

Phases in fetal brain development

UCSF

- 19-26 GA
 - Layers well delineated in all cortical regions.
- 27-30 GA: developmental peak
 - Subplate zone/white matter border becomes less distinct.
- 30+ GA
 - germinal matrix and the subplate zone gradually disappear
- 31-36 GA: subplate dissolution
 - disappears from primary cortical areas
 - very thin around the cortical sulci.



-> Transient laminar pattern transforms into mature-like structure of the cerebral wall (cortex, white matter, corona radiata, centrum semi-ovale).

-> Different Analysis Approaches Required for different stages

33

Tissue Contrast in Fetal MRI and the need for Spatial Priors in Segmentation

UCSF

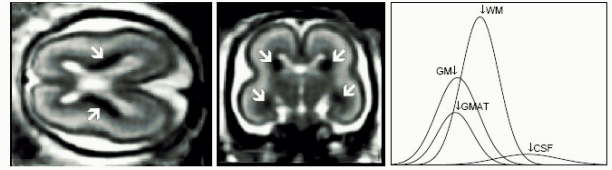
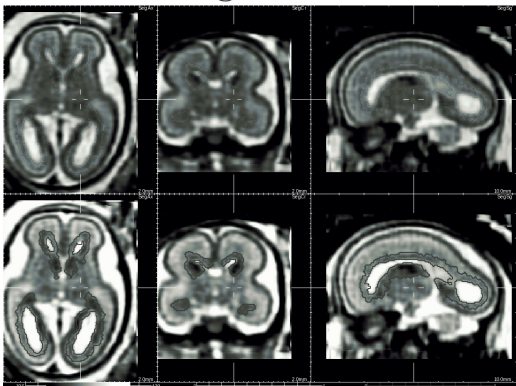


Fig. 1. Axial and coronal views of an MR T2w image with clearly visible hypointense regions of the germinal matrix. Distribution of voxel intensities for grey matter (GM), the germinal matrix (GMAT), white matter (WM), and cerebrospinal fluid (CSF).

34

Manual Tracing of Germinal Matrix

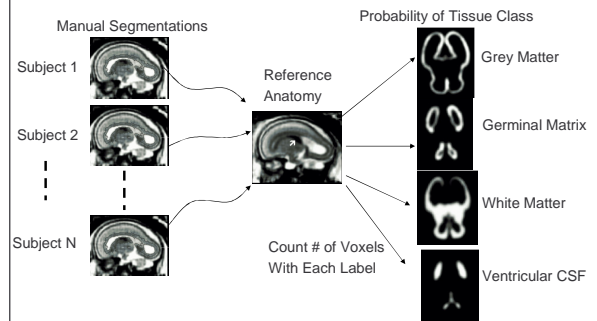
UCSF



35

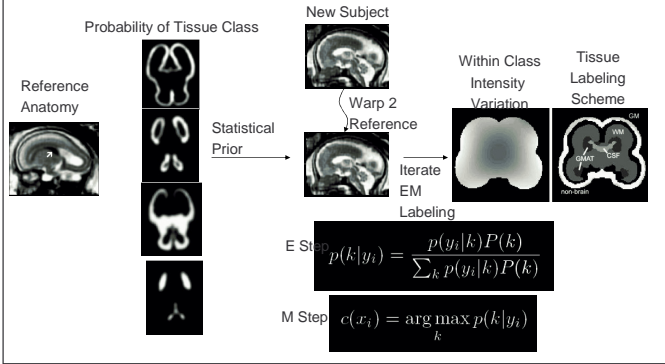
Statistical Model of Developing Tissue Distribution

UCSF

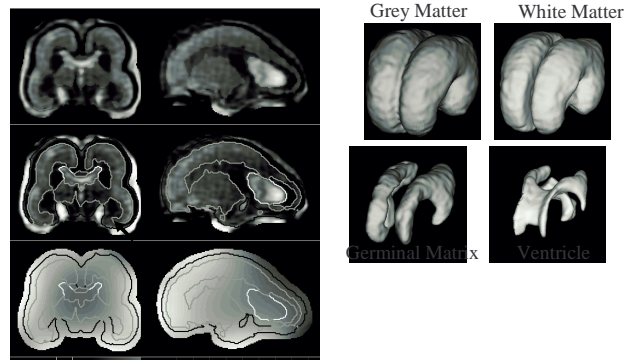


36

EM Segmentation of Developing and Developed Tissues



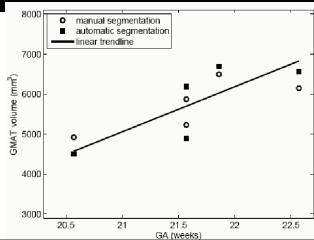
Example Tissue Labeling



Tissue Volume Validation

Table 1. Volumes of brain tissues (in mm³) for fetal subjects of different gestational age (GA, in weeks) obtained from automatic and manual segmentation.

Fetus	GA	automatic segmentation				man. seg.	rel. diff.
		CSF	GM	WM	GMAT	GMAT	
A	20.57	3155	13436	10287	4497	4920	8.6%
B	21.57	2831	13985	10555	4892	5229	6.4%
C	21.57	3588	18543	20549	6186	5872	5.3%
D	21.86	3223	20523	20215	6685	6405	2.9%
E	22.57	3894	18834	25339	6561	6146	6.7%



Cortical Thickness Measurements in Fetal MRI

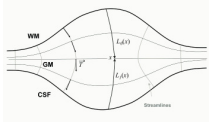
Defining and Measuring Cortical Thickness

UCSF

Problem of defining a unique measure of thickness!

Addressed in adult image analysis

eg [S. E. Jones, B. R. Buchbinder, and I. Aharon, "Three-dimensional mapping of cortical thickness using Laplace's equation," Hum. Brain Mapp. 11(1), pp. 12-32, 2000.]



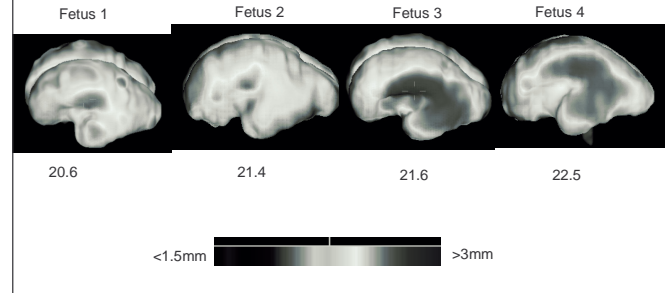
- Thickness defined as the length of a streamline through point "x" in gray matter region
- Streamline defined as trajectory tangent to the normalized gradient (T) of a harmonic scalar

$$\nabla^2 \Psi = \frac{\partial^2 \Psi}{\partial x^2} + \frac{\partial^2 \Psi}{\partial y^2} + \frac{\partial^2 \Psi}{\partial z^2} = 0$$

41

Preliminary Cortical Thickness Results

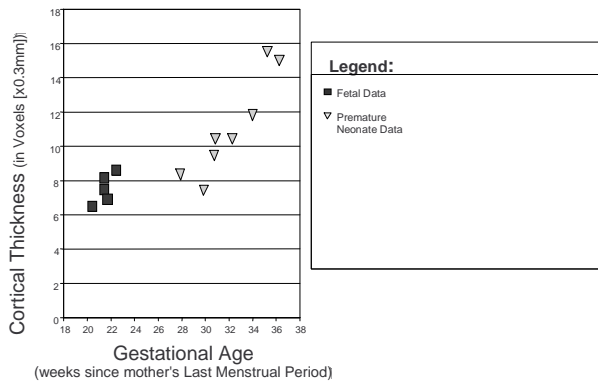
UCSF



42

Mean Cortical Thickness vs. Gestational Age

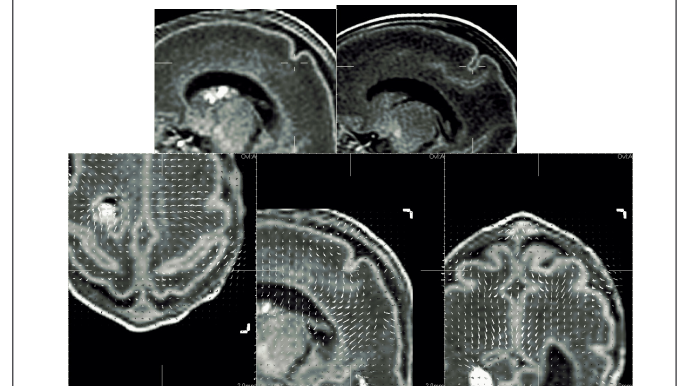
UCSF



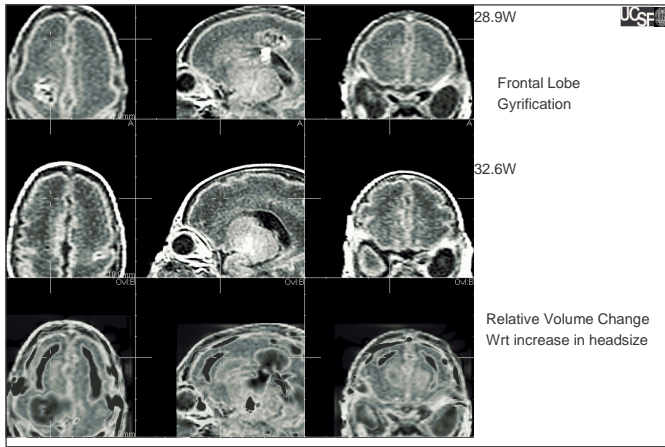
43

Mapping Patterns of Brain Growth in Premature Babies

UCSF



44



Summary

- 3D Fetal Brain Image Analysis is Possible!
- Can Correction Fetal Motion present in Clinical Studies and form a 3D volume image
- Tissue Segmentation techniques can be extended
 - To include transient and developed tissue types
- Cortical Thickness estimation from reconstructed MRI data shows promising results
 - Need to develop models of pattern vs age

Acknowledgements

NIH/NINDS R01-NS055064

- Biomedical Image Computing Group
 - Dr Kio Kim, Dr Piotr Habas, Dharshan Chandramohan
- Clinical Collaborators at UCSF
 - Dr Orit Glenn, Dr A.J. Barkovich, Dr Donna Ferriero